Piezoelectric non-linearity in  $\text{PbSc}_{0.5}\text{Ta}_{0.5}\text{O}_3$  thin filmsAnuj Chopra<sup>a,b,\*</sup>, Yunseok Kim<sup>a,c</sup>, Marin Alexe<sup>a,d</sup>, Dietrich Hesse<sup>a</sup><sup>a</sup> Max Planck Institute of Microstructure Physics, Weinberg 2, D-06120 Halle (Saale), Germany<sup>b</sup> Faculty of Science and Technology, MESA+ Institute for Nanotechnology, University of Twente, P.O. Box 217, 7500 AE Enschede, The Netherlands<sup>c</sup> School of Advanced Materials Science and Engineering, Sungkyunkwan University (SKKU), Suwon 440-746, Republic of Korea<sup>d</sup> Department of Physics, University of Warwick, Coventry CV4 7AL, UK

## ARTICLE INFO

## Article history:

Received 31 March 2014

Received in revised form

21 May 2014

Accepted 4 June 2014

Available online 21 June 2014

## Keywords:

A. Thin films

B. Epitaxial growth

D. Dielectric properties

D. Ferroelectricity

D. Piezoelectricity

## ABSTRACT

Epitaxial (001)-oriented  $\text{PbSc}_{0.5}\text{Ta}_{0.5}\text{O}_3$  (PST) thin films were deposited by pulsed laser deposition. Local piezoelectric investigations performed by piezoelectric force microscopy show a dual slope for the piezoelectric coefficient. A piezoelectric coefficient of 3 pm/V was observed at voltages up to 0.8 V. However, at voltages above 0.8 V, there is a steep increase in piezoelectric coefficient mounting to 23.2 pm/V. This nonlinear piezoelectric response was observed to be irreversible in nature. In order to better understand this nonlinear behavior, voltage dependent dielectric constant measurements were performed. These confirmed that the piezoelectric non-linearity is indeed a manifestation of a dielectric non-linearity. In contrast to classical ferroelectric systems, the observed dielectric non-linearity in this relaxor material cannot be explained by the Rayleigh model. Thus the dielectric non-linearity in the PST films is tentatively explained as a manifestation of a percolation of the polar nano regions.

© 2014 Elsevier Ltd. All rights reserved.

## 1. Introduction

Relaxors have been instrumental in attaining several applications through the years. There has been a recent resurgence of interest in relaxor ferroelectrics because of their prospective use as actuators, switches and security systems [1–3]. Among them,  $\text{PbSc}_{0.5}\text{Ta}_{0.5}\text{O}_3$  (PST) is one of the well-known ferroelectric relaxors which is a potential candidate for IR-detection due to its high figure of merit [4,5]. PST crystallizes in the perovskite structure with the compositional formula  $\text{A}(\text{B}'\text{B}'')\text{O}_3$ , where the A sites are occupied by  $\text{Pb}^{2+}$  cations and the B sites are statistically shared by  $\text{Sc}^{3+}$  and  $\text{Ta}^{5+}$  cations. As the devices are designed to work under the application of an applied external electric field, it is very important to understand the influence of such an external field on the piezoelectric and dielectric behavior of the relaxor material, so that the performance of relaxor-built devices can be understood completely. Piezoelectric and dielectric nonlinearities are quite well known for ferroelectrics. In this regard, several phenomenological models have been suggested, yet a full description of these nonlinear properties is still lacking [6–9]. Dielectric and piezoelectric responses of a normal ferroelectric material are due to intrinsic and extrinsic contributions. The former one comes from

the deformation of the unit cell, caused by the application of the electric field [10,11]. The latter contribution is a response of the domain wall motion due to the applied electric field. The intrinsic nonlinearity can be modeled and explained by free energy equations and the Landau–Ginzburg–Devonshire theory [12,13]. However, the extrinsic nonlinearity, which has a complex physical origin such as pinning, de-pinning and re-pinning of domain walls during domain wall motion, is difficult to quantify [8]. In this paper, we report on irreversible and strong piezoelectric non-linearity well below the coercive voltage, in PLD-prepared thin PST films. The obtained results and their analysis indicate that the observed piezoelectric non-linearity is a manifestation of the percolation of polar nanoregions (PNRs) in thin PST films.

## 2. Experimental procedure

(001)-oriented PST thin films were deposited on  $\text{La}_{0.7}\text{Sr}_{0.3}\text{MnO}_3$  (LSMO)-electroded STO substrates by ablating a self-prepared PST target with KrF excimer laser pulses (wavelength of 248 nm, duration 20 ns). In order to achieve  $\text{TiO}_2$ -terminated surfaces, vicinal STO (0 0 1) substrates (0.1° offcut; from CrysTec GmbH, Berlin) were chemically treated and annealed at a temperature of 1000 °C before loading into the deposition chamber. For the electrical measurements, a 60 nm thick epitaxial LSMO layer was deposited as a bottom electrode with 5 Hz repetition rate and a fluence of 2 J/cm<sup>2</sup>. The bottom electrode was deposited at optimized

\* Corresponding author at: Faculty of Science and Technology, MESA+ Institute for Nanotechnology, University of Twente, P.O. Box 217, 7500 AE Enschede, The Netherlands. Tel.: +31 53 4892989; fax: +31 53 4892990.

E-mail address: [anujchopraiitm@gmail.com](mailto:anujchopraiitm@gmail.com) (A. Chopra).

growth temperature and oxygen pressure of 650 °C and 0.141 mbar, respectively. PST films were deposited at 550 °C with 0.270 mbar oxygen pressure. More details on the PST growth conditions can be found elsewhere [14–18]. After the deposition, the films were cooled down to room temperature with a slow cooling rate of 5 °C/min in 1 bar oxygen pressure. In order to facilitate electrical measurements, Pt top electrodes with a size of  $60 \times 60 \mu\text{m}^2$  area were sputtered by radio frequency sputtering at room temperature through a shadow mask.

Crystallographic characterizations were performed by a Philips X'Pert MRD X-ray diffractometer with Cu  $K\alpha$  ( $\lambda=0.15418 \text{ nm}$ ) radiation. Samples for transmission electron microscopy (TEM) were prepared using mechanical and ion-beam based standard techniques. TEM images were recorded on a Philips CM20T operated at 200 kV. Surface morphology and local polarization switching were investigated by a commercial atomic force microscope (AFM) (XE-100, Park Systems), using the piezoresponse force microscopy (PFM) mode. Dielectric constants were calculated from the capacitance measured by a Hewlett Packard 4194 A impedance analyzer.

### 3. Results and discussions

The out-of-plane XRD pattern obtained for a PST/LSMO/STO heterostructure is shown in Fig. 1(a). Both PST and LSMO films are (001)-oriented as shown in the  $\theta$ -2 $\theta$  scan. The out-of-plane lattice parameter of the PST film has been calculated using the XRD diffraction pattern and it was found to be 4.08 Å which is slightly higher than the bulk lattice parameter [19]. The  $\phi$ -scan (in-plane) scans for STO, LSMO and PST contain four peaks (Fig. 1(b)) for each material at the same azimuthal angle ( $\phi$ ), revealing that all the films have epitaxial cube-on-cube growth. The in-plane and out-of-plane epitaxial relationships between substrate (STO), electrode layer (LSMO) and PST thin film have been found to be (001) PST// (001) LSMO// (001) STO and [100] PST//[100] LSMO//[100] STO, respectively (cubic indexing is used for LSMO and PST). The full width at half maximum values (FWHM) of the (222) reflections for STO, LSMO, and PST were found to be  $\sim 0.29^\circ$ ,  $0.30^\circ$ , and  $0.60^\circ$  respectively, confirming a good crystalline growth. The surface morphology and roughness of the PST thin film were investigated by AFM measurements. The surface morphology of a PST film deposited on a vicinal STO substrate (Fig. 2(a)) is shown in Fig. 2(b), and reveals a smooth surface morphology. The PST films have

a root mean square value of roughness of about 0.6 nm over an area of  $4 \times 4 \mu\text{m}^2$  signifying a flat and smooth surface of the PST film on LSMO/STO. However, due to large lattice mismatch (4.91%) between STO and PST, no step patterns were observed for PST films.

The microstructure of the PST thin films was investigated by TEM. The cross-sectional TEM image (Fig. 3(a)) and the selected area diffraction (SAED) pattern (Fig. 3(b)) (only indexed for PST) captured along the [110] direction reveal the epitaxial growth of the 30 nm thick PST film on a 65 nm thick LSMO bottom electrode. Detailed cross-sectional TEM investigations indicate a coherent growth of the LSMO layer on the STO substrate due to the very small lattice mismatch (0.6% at RT), whereas the PST film shows a columnar type of growth, possibly due to the large lattice mismatch (4.91%). The in-plane and out-of-plane lattice parameters for the 30 nm thin PST film were calculated through SAED patterns as shown in Fig. 3(c). For a cubic PST system, the ratio between AB/BC and the angle between AB and BE vectors should be 1.41 and  $35.26^\circ$ , respectively. The observed values of the ratio between AB/BC and the angle between AB and BE vectors were found to be 1.43 and  $33.90^\circ$  respectively which indicate that the PST film is tetragonally distorted.

The ferroelectric switching of the PST films has been locally investigated with a modulation voltage of 0.7 V<sub>rms</sub> at 25 kHz by PFM, as shown in Fig. 4(a). A  $3 \times 3 \mu\text{m}^2$  area was poled downwards by applying a voltage of +5 V for background poling and then, at the center, a smaller area of  $1 \times 1 \mu\text{m}^2$  was switched upwards by applying a voltage of −5 V. This reveals that the films can be locally switched in either direction by applying an external voltage. The locally switched area of the films remained unchanged (Fig. 4(b)) for more than one hour for relaxor PST, suggesting that the films have decent retention characteristics. The piezoresponse of a PST film was investigated as a function of the applied ac voltage (25 kHz) using PFM measurements as shown in Fig. 4(c). When the piezoelectric coefficient primarily contributes to the amplitude of the PFM signal, the amplitude of the PFM signal is a linear function of the applied voltage for  $V_{ac}$  lower than the corresponding coercive voltage. Thus, the piezoresponse data can be linearly fitted to approximate the effective piezoelectric coefficient. However, for a  $V_{ac}$  value at and above the coercive voltage, the PFM signal drops significantly because of the change of direction of the polarization. Interestingly, even below the coercive voltage ( $V_c$ ), two slopes, instead of obtaining one single slope, were observed for the PST film as shown in Fig. 4(c). The piezoelectric coefficient in the low

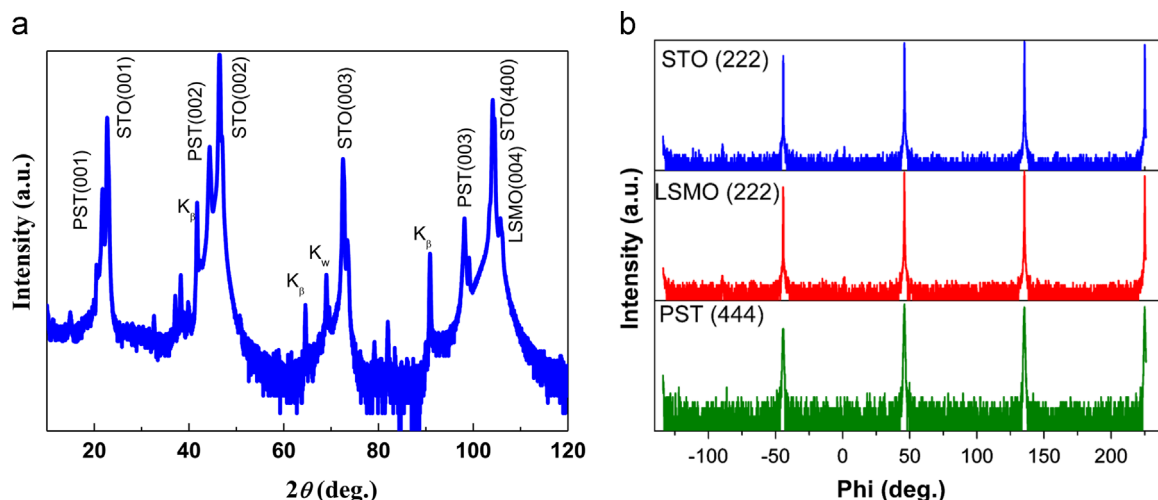


**Fig. 1.** (a) XRD  $\theta$ -2 $\theta$  scan recorded for a (001)-oriented PST/LSMO/STO heterostructure revealing that the films are in pure perovskite phase. (b) A  $\phi$ -scan performed using the (444) reflections of PST, and the (222) reflection of the LSMO electrode and STO substrate confirming epitaxial cube-on-cube growth.

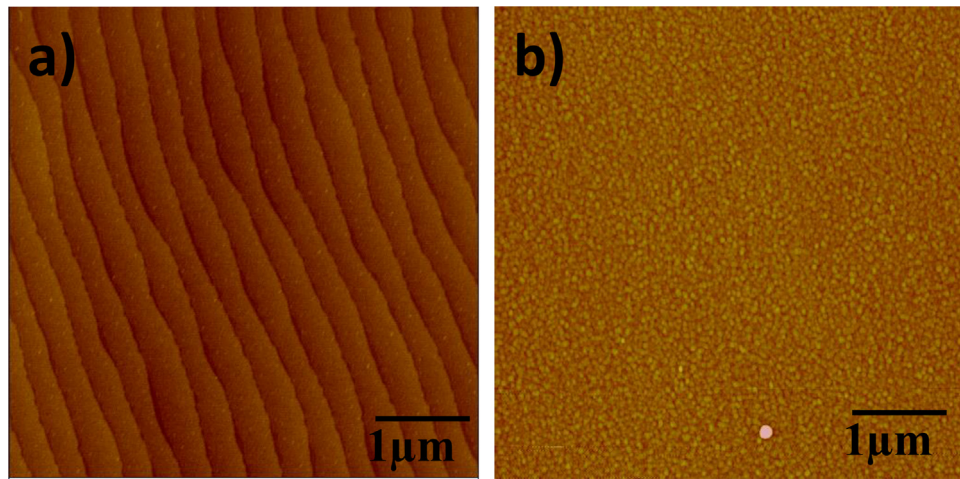


**Fig. 2.** AFM images of a  $4 \times 4 \mu\text{m}^2$  area recorded for (a) an etched and subsequently annealed STO (001) substrate, showing unit cell-high steps and terraces, and (b) a 30 nm thick PST thin film.

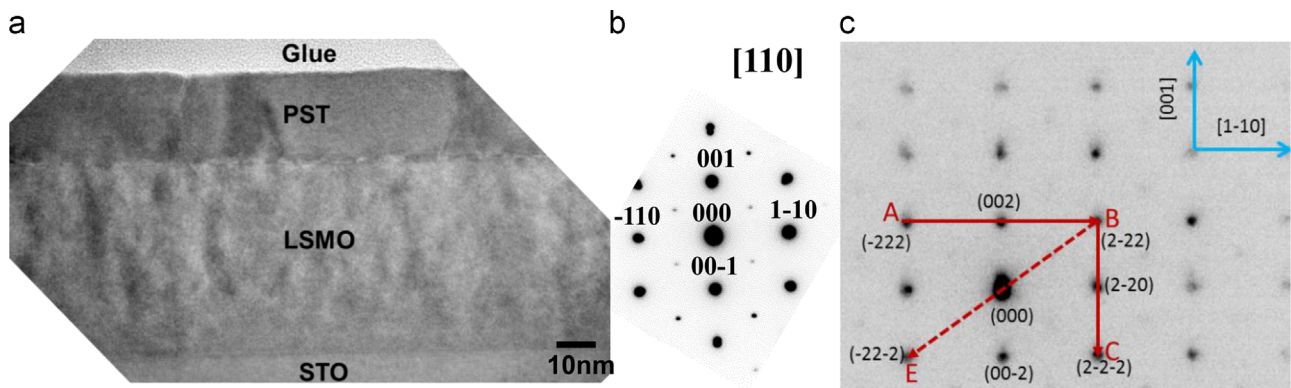


**Fig. 3.** (a) A cross-section image of a PST(001)/LSMO(001)/STO(001) heterostructure recorded along the [110] direction. (b) Cross-sectional SAED pattern showing that all the films are epitaxial. (c) SAED pattern of PST films in [110] direction confirming that the PST film is tetragonal.

voltage range ( $< 0.8 \text{ V}$ ) is  $3 \text{ pm/V}$ , and a sharp increase in the piezoresponse is observed for voltages higher than  $0.8 \text{ V}$ . In other words, a higher piezoelectric coefficient is observed for the high voltage regime. The coercive voltage for PST films is found to be  $1.7 \text{ V}$  as shown in the inset of Fig. 4(c). It is also observed that the piezoresponse never comes back to the lower value after applying an ac voltage higher than  $0.8 \text{ V}$ , but instead remains always higher than the pristine value after the application of a high voltage as shown in Fig. 5(a).

The piezoelectric coefficient for a (001) ferroelectric material with tetragonal symmetry can be given as [20,21]

$$d_{33} = 2\epsilon_{33}Q_{33}P_{33}^s$$

where  $d_{33}$ ,  $\epsilon_{33}$ ,  $Q_{33}$  and  $P_{33}^s$  are the longitudinal piezoelectric coefficient, the dielectric permittivity, the electrostriction coefficient and the vertical component of the spontaneous polarization, respectively. Thus, the PFM amplitude can be influenced by three factors: dielectric constant, polarization, and electrostriction coefficient. Since the electrostriction coefficient is expected to follow a quadratic relationship with the applied voltage, the electrostriction may not primarily contribute to the observed phenomenon. Furthermore, since the applied voltage range is well below the coercive voltage, significant polarization switching is not expected. In order to check the possibility of a change in the dielectric constant with applied voltage, the voltage-dependent dielectric constant was measured. Similar to the piezoresponse measured by PFM, a sharp increase in the dielectric constant was observed around  $\sim 0.6 \text{ V}$  for  $1 \text{ kHz}$  as shown in Fig. 5(b). The dielectric

constant changes irreversibly to a value higher than the pristine value. However, no change in dielectric losses was observed. The dielectric constant for the pristine sample at  $0.1 \text{ V}$  was found to be 407 and after exposing the sample to a cycle of higher  $V_{ac}$  voltages, and returning to  $0.1 \text{ V}$ , it increased to 410 (Fig. 5(b)). The voltages at which the slope of the dielectric constant and that of the piezoelectric coefficient change were found to be quite close. However, the change in the pristine value of the piezoelectric coefficient is small as compared to the value of the dielectric constant. In case of piezoresponse measurements, the response is local and thus it might be from a region which responds faster to the applied voltage as compared to other regions in the sample. Dielectric constant measurements are rather global, thus the average response might be lower than the piezoelectric response. Thus, it is corroborated that a dielectric non-linearity is probably responsible for the nonlinear piezoelectric behavior.

The dielectric non-linearity is already reported in literature for few ferroelectric materials [6–9]. In this context, several phenomenological models have been proposed to explain the physical origin of the dielectric and piezoelectric anomalies [11,22,23]. Nevertheless, none of these models have gained universal acceptance yet, due to some contradictory experimental results [24–26]. The Rayleigh model is used to explain the dielectric non-linearity on the basis of reversible and irreversible domain wall motion under applied external bias [27,28]. In contrast to normal ferroelectrics, relaxors do not have classical ferroelectric domains, thus the idea of dielectric nonlinearity due to domain wall motion in relaxors is ambiguous. The Rayleigh model is not valid in the high



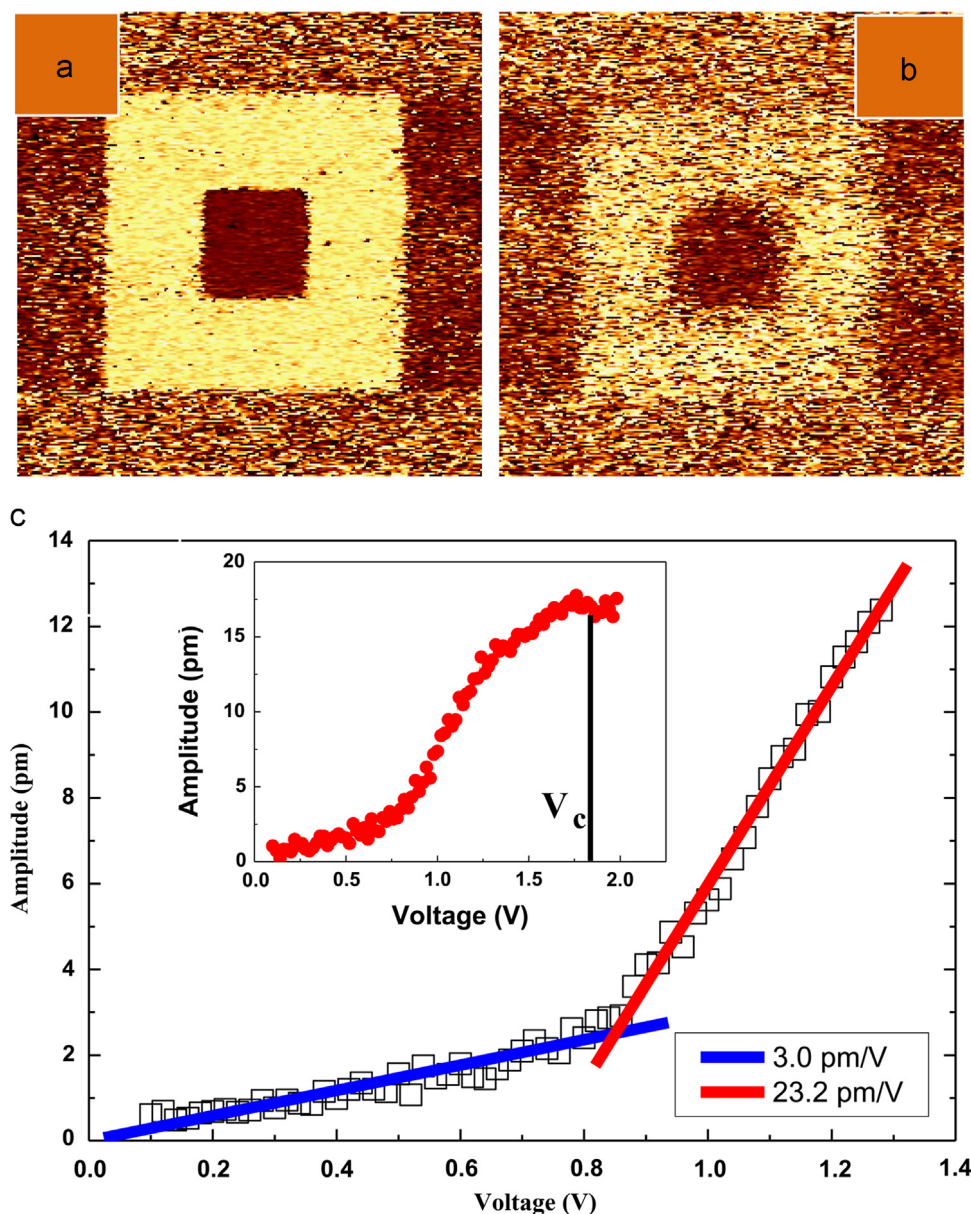


**Fig. 4.** (a and b) PFM phase images ( $5 \times 5 \mu\text{m}^2$ ) of a 30 nm thick PST film: (a) after box patterned poling by application of  $\pm 5$  V and (b) after 1 h revealing quite a good retention characteristics. (c) Piezoresponse of the PST film as a function of the  $V_{ac}$  excitation voltage. The inset shows the PFM signal at higher voltage with a strong non-linear behavior at coercive voltage ( $V_c$ ).

voltage region, however, the ferroelectric loop ( $P$ - $V$ ) and ( $I$ - $V$ ) measurements at voltages lower than 1.5 V show almost no switching current indicating that we are well below the high voltage region, as shown in Fig. 6. The ferroelectric hysteresis loops were measured at 1 kHz frequency. The coercive voltage values for PST films and bulk are almost same and are found to be  $\sim 1.5$  V [29]. In addition, according to the Rayleigh model, the non-linearity is reduced with increase in frequency [6,30]. But in our case no frequency dependence was observed as shown in variation of slope of dielectric constant with frequency in Fig. 7. Thus, the observed dielectric non-linearity cannot be explained using the Rayleigh model. In order to address the observed dielectric non-linearity in PST films, the possibility of a field-induced phase transition was explored, however no such phenomenon was experimentally observed.

Percolation of polar nano regions (PNRs) is quite well known in relaxors [31–35]. We propose the possibility of percolation of PNRs

after a certain threshold voltage, which facilitates the PNRs to interact with each other. As the voltage is removed, most of the PNRs might return back to the ergodic phase while few PNRs remain intact at their positions. Possibly, the intact clusters of PNRs are responsible for the irreversibility of the dielectric and piezoelectric properties. However, further detailed investigations and models will be required to understand this non-linearity behavior in PST thin films, before they can be used for applications.

In summary, tetragonally distorted 30 nm thin epitaxial PST films were deposited on LSMO-electroded STO substrates. A sudden increase of the piezoelectric response is observed for voltages higher than 0.8 V which is found to be the manifestation of a dielectric non-linearity. The observed dielectric non-linearity is tentatively explained as a result of a percolation of the polar nanoregions. New theories will have to emerge in order to comprehensively understand the non-linear dielectric and piezoelectric behavior of relaxor-type ferroelectric films.

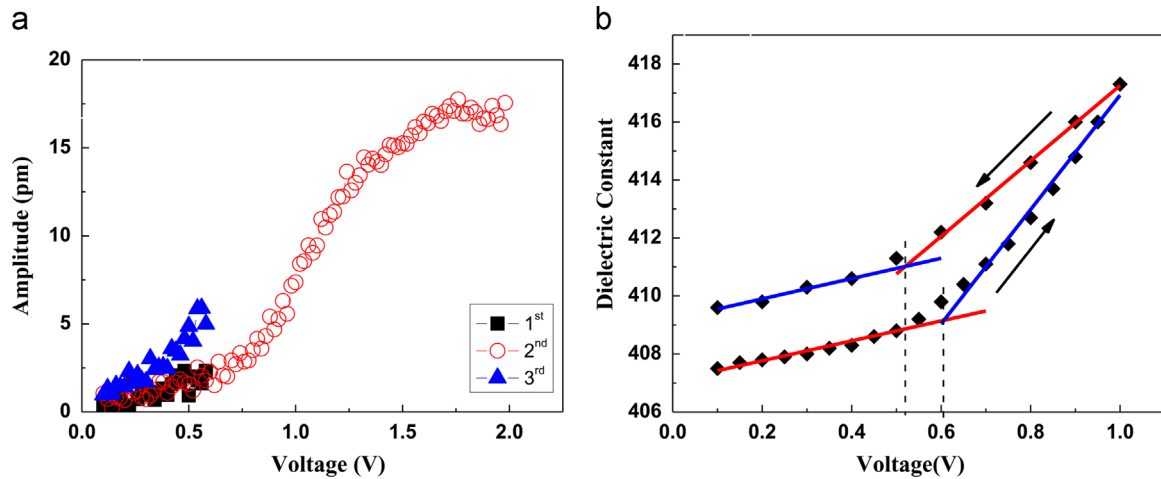


Fig. 5. (a) Piezoresponse of the PST film as a function of the applied ac voltage showing an increase in the piezoelectric coefficient for the 3rd cycle. (b) Dielectric constant variation of the PST film as a function of the applied ac voltage showing a sharp increase in dielectric constant at 0.6 V.

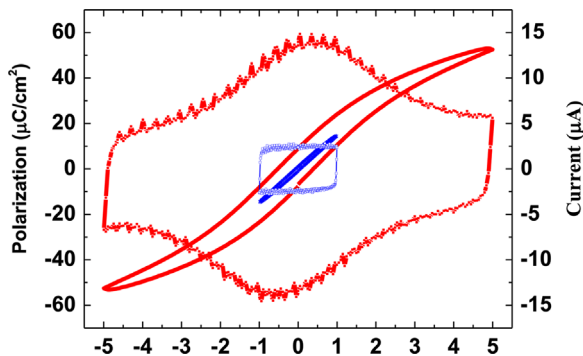


Fig. 6. Macroscopic polarization-voltage and switching current-voltage hysteresis curves of a PST film at RT. The PST film shows no switching characteristics below 1.5 V.

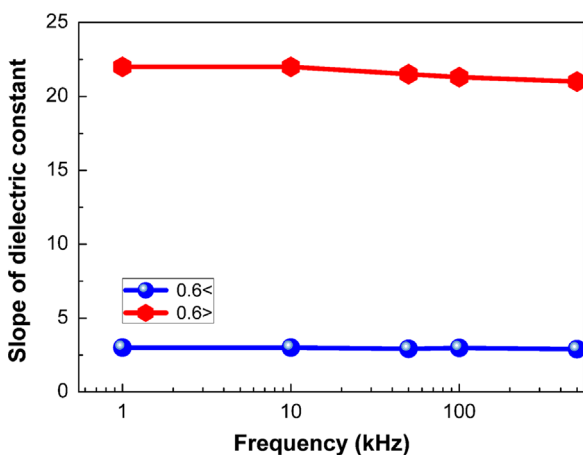


Fig. 7. Variation of slope of dielectric constant with frequency. The blue color points show the slopes measured below 0.6 V and red color points are above it. (For interpretation of the references to color in this figure legend, the reader is referred to the web version of this article).

## Acknowledgments

The authors would like to thank Ms. M. Herrmann for TEM sample preparation, and Mr. N. Schammelt for PLD system maintenance. This work was funded by DFG via SFB 762.

## References

- [1] R.E. Cohen, *Nature* 441 (2006) 22.
- [2] K. Uchino, *Ferroelectrics* 151 (1994) 321.
- [3] S.E. Park, T.R. Shrout, *Mater. Res. Innov.* 1 (1997) 20.
- [4] R.W. Whatmore, *Ferroelectrics* 118 (1991) 241.
- [5] N.M. Shorrocks, R.W. Whatmore, P.C. Osbond, *Ferroelectrics* 106 (1990) 387.
- [6] N.B. Gharb, I. Fujii, E. Hong, S.T. McKinstry, D.V. Taylor, D. Damjanovic, *J. Electroceram.* 19 (2007) 49.
- [7] N.B. Gharb, S.T. McKinstry, D. Damjanovic, *J. Appl. Phys.* 100 (2006) 044107.
- [8] D.A. Hall, *J. Mater. Sci.* 36 (2001) 4575.
- [9] V.V. Shvartsman, N.A. Pertsev, J.M. Herrero, C. Zaldo, A.L. Kholkin, *J. Appl. Phys.* 97 (2005) 104105.
- [10] R.E. Eitel, T.R. Shrout, C.A. Randall, *J. Appl. Phys.* 99 (2006) 124110.
- [11] D.V. Taylor, D. Damjanovic, *Appl. Phys. Lett.* 73 (1998) 2045.
- [12] L. Chen, V. Nagarajan, R. Ramesh, A.L. Roytburd, *J. Appl. Phys.* 94 (2003) 5147.
- [13] M. Budimir, D. Damjanovic, N. Setter, *Appl. Phys. Lett.* 85 (2004) 2890.
- [14] A. Chopra, B.I. Birajdar, A. Berger, M. Alexe, D. Hesse, *J. Appl. Phys.* 114 (2013) 224109.
- [15] A. Chopra, B.I. Birajdar, Y. Kim, I. Vrejoiu, M. Alexe, D. Hesse, *Appl. Phys. Lett.* 95 (2009) 022907.
- [16] B.I. Birajdar, A. Chopra, M. Alexe, D. Hesse, *Acta Mater.* 59 (2011) 4030.
- [17] A. Chopra, D. Pantel, Y. Kim, M. Alexe, D. Hesse, *J. Appl. Phys.* 114 (2013) 084107.
- [18] A. Chopra, B.I. Birajdar, A. Berger, M. Alexe, D. Hesse, *New J. Phys.* 16 (2014) 013059.
- [19] P. Groves, *J. Phys. C* 18 (1985) L1073.
- [20] A. Gruverman, O. Auciello, H. Tokumoto, *Integr. Ferr.* 19 (1998) 49.
- [21] Y. Kim, A. Kumar, A. Tselev, I.I. Kravchenko, H. Han, I. Vrejoiu, W. Lee, D. Hesse, M. Alexe, S.V. Kalinin, S. Jesse, *ACS Nano* 5 (2011) 9104.
- [22] P. Bintachitt, S. Jesse, D. Damjanovic, Y. Han, I.M. Reaney, S.T. McKinstry, S.V. Kalinin, *Proc. Natl. Am. Soc.* 107 (2010) 7219.
- [23] G. Robert, D. Damjanovic, N. Setter, A.V. Turik, *J. Appl. Phys.* 89 (2001) 5067.
- [24] A.K. Tangsev, A.E. Glazounov, *Phys. Rev. B* 57 (1998) 18.
- [25] D. Kobor, A. Hajjaji, J.E. Garcia, R. Perez, A. Albareda, L. Lebrun, D. Guyomar, *J. Mod. Phys.* 1 (2010) 211.
- [26] J.E. Garcia, R. Perez, A. Albareda, *J. Phys.: Condens. Matter* 17 (2005) 7143.
- [27] D.A. Hall, P.J. Stevenson, *Ferroelectrics* 228 (1999) 139.
- [28] D.A. Hall, *Ferroelectrics* 223 (1999) 319.
- [29] N. Setter, L.E. Cross, *J. Appl. Phys.* 51 (1980) 4356.
- [30] T. Tsurumi, K. Soejima, T. Kamiya, M. Daimon, *Jpn. J. Appl. Phys.* 33 (1994) 1959.
- [31] S.E. Lerner, P.B. Ishai, A.J. Agranat, Y. Feldman, *J. Non-Cryst. Solids* 353 (2007) 4422.
- [32] C.S. Tu, R.R. Chien, C.M. Hung, V.H. Schmidt, F.T. Wang, C.T. Tseng, *Phys. Rev. B* 75 (2007) 212101.
- [33] E. Dulkun, M. Roth, B. Dkhil, J.M. Kiat, *J. Appl. Phys.* 98 (2005) 023520.
- [34] L.S. Kamzina, A.L. Korzhenevskii, *Ferroelectrics* 131 (1992) 91.
- [35] V.Y. Shur, G.G. Lomakin, V.P. Kuminov, D.V. Pelegov, S.S. Beloglazov, S.V. Slavikovskii, I.L. Sorkin, *Phys. Solid State* 41 (1999) 453.